Chapter 4
Homochirality: a prerequisite or consequence of life?

Axel Brandenburg

Abstract Many of the building blocks of life such as amino acids and nucleotides are chiral, i.e., different from their mirror image. Contemporary life selects and synthesizes only one of two possible handednesses. In an abiotic environment, however, there are usually equally many left- and right-handed molecules. If homochirality was a prerequisite of life, there must have been physical or chemical circumstances that led to the selection of a certain preference. Conversely, if it was a consequence of life, we must identify possible pathways for accomplishing a transition from a racemic to a homochiral chemistry. After a discussion of the observational evidence, we review ideas where homochirality of any handedness could emerge as a consequence of the first polymerization events of nucleotides in an emerging RNA world. These mechanisms are not limited to nucleotides, but can also occur for peptides, as a precursor to the RNA world. The question of homochirality is, in this sense, intimately tied to the origin of life. Future Mars missions may be able to detect biomolecules of extant or extinct life. We therefore also discuss possible experimental setups for determining the chirality of primitive life forms in situ on Mars.

Key words: DNA polymerization, enantiomeric cross-inhibition, origin of homochirality. Revision: 1.80

[1]Nordita, KTH Royal Institute of Technology and Stockholm University, Stockholm, Sweden
[2]Department of Astronomy, AlbaNova University Center, Stockholm, Sweden
[3]McWilliams Center for Cosmology, Carnegie Mellon University, Pittsburgh, PA 15213, USA
Correspondence: Nordita, Hannes Alfvéns väg 12, SE-10691 Stockholm, Sweden
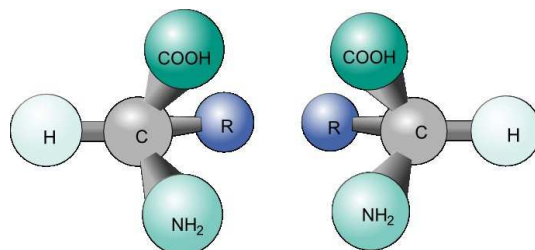e-mail: brandenb@nordita.org, Tel: +46 8 5537 8707, mobile: +46 73 270 4376
http://orcid.org/0000-0002-7304-021X

Fig. 4.1 An amino acid that is chiral whenever the residue R is different from H. For example, when R = CH$_3$, we have alanine, but when R = H, the molecule is glycine, which is the same as its mirror image, i.e., it is achiral. (Source: `https://chem.libretexts.org/@api/deki/files/19089/molecule.png?revision=1`)

4.1 Introduction

The occurrence of handedness in biology is not uncommon. The difference between our left and right hands is the most obvious occurrence in the macroscopic world. In ancient Greek, the word $\chi\epsilon\iota\rho$ means hand, which explains the origin of the word chirality. Also some trees exhibit a preference for a left-handed swirl and others for a right-handed swirl. Snails are another such example. In the microscopic world, the biological significance of a preferred handedness was discovered by Pasteur (1853) by analyzing the effect of tartaric acid on polarized light.

Polarization is a property of transversal waves when the wave shows oscillations perpendicular to the direction of propagation. This is different for sound waves that are longitudinal. Unpolarized light consists of a superposition of waves with all the different polarization orientations of the wave plane. Using a polarizer, which is an optical filter with maximum transmission for a particular wave plane, one can determine the orientation of polarization. It turns out that natural sugar in solution has the property of rotating the plane of polarization of polarized light in the right-handed sense, so they are called dextrorotatory, denoted by (+), while many amino acids in solution rotate polarized light in the left-handed sense, denoted by (−). Pasteur (1853) also inspected the shapes of crystals of tartaric acid under the microscope and found upon separating them that the two rotate polarized light in opposite senses.

Handedness of biomolecules is primarily a consequence of the tetrahedral shape of the of carbon compounds; see Figure 4.1. If each of the four bonds of the carbon atom connect to a different group, its three dimensional structure would be different from that of its mirror image. In the case of complex molecules, there can be several carbon atoms that cause a violation of mirror symmetry. Those carbon atoms are then called chiral centers. In the case of tartaric acid (Figure 4.2), there are two chiral centers. There is then also the
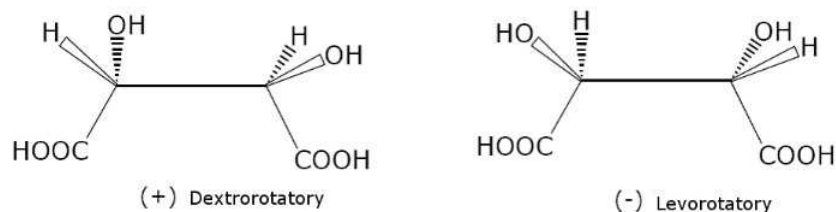
Fig. 4.2 Dextrorotatory (left) and levorotatory (right) tartaric acid. Adapted from Sevin (2015).

possibility that only one of the two chiral centers is different. That version is called meso-tartaric acid and it is achiral, i.e., it is mirrorsymmetric.

There is no immediate connection between the handedness of molecules (Figure 4.2) and the handedness hidden in the structure of a crystal (Figure 4.3). In fact, the association of a given chiral structure with left or right relies on some convention. This also explains that there is nothing strange in having right-handed sugars in our DNA and left-handed amino acids in our proteins. Nevertheless, the very fact that something can occur in two possible forms that are mirror images of one another is non-trivial and requires some underlying structure that can also be subdivided into two opposite mirror images of each other. It is therefore plausible that one of the two handednesses of the L-tartaric acid molecule crystallizes into macroscopic structures of one form, and the D-tartaric acid into its mirror image (Derewenda, 2008). In the molecular context, these two forms are called enantiomers.[1]

Interestingly, already back then, Pasteur made the statement that the occurrence of handedness is a demarcating property between living and non-

[1] We must emphasize that the terminology in terms of levorotatory and dextrorotatory is quite different from that in terms of D and L. Levorotatory/dextrorotatory is the physical property for a compound to induce the rotation of polarized light to the left/right. This property is abbreviated $(-)/(+)$. By contrast, L/D refers to a structural property of a molecule to denote its handedness, that is solely based on conventions. This convention only applies to specific biomolecules, including amino acids and sugars. This convention has been taken in such a way that all biogenic sugars are D, and all biogenic amino acids are L. There is yet another terminology in which R and S refer to a structural property denoting the handedness of a given chiral carbon in a molecule. This is also based on a convention, which applies to any chiral organic compound. This convention has been taken in such a way that any chiral carbon can be assigned uniquely an R or S handedness given a precise set of rules and is thus a drastically different convention from L/D. For example, biogenic L-alanine is dextrorotatory $(+)$ and its chiral carbon is of configuration S; biogenic L-serine is levorotatory $(-)$ and its chiral carbon is of configuration S; biogenic L-cysteine is dextrorotatory $(+)$ and its chiral carbon is of configuration R. Regarding sugars, D-glucose is dextrorotatory and D-fructose is levorotatory. Note also that common table sugar (sucrose, i.e., a D-glucose–D-fructose dimer) is dextrorotatory. If one hydrolyzes it, one obtains a 1:1 mixture of D-glucose:L-fructose, corresponding to a mixture that is levorotatory, and thus its common name of "inverted sugar".
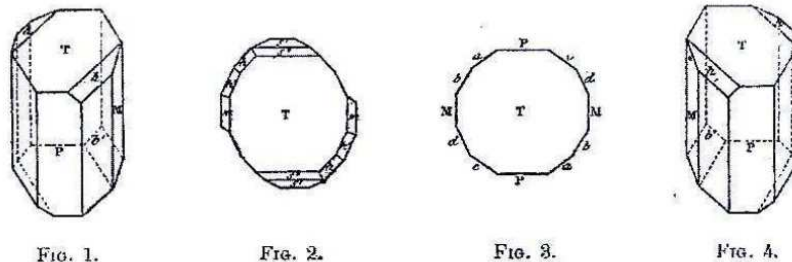
Fig. 4.3 Original drawing from Pasteur's publication (Pasteur, 1922) showing dextroro-tatory (left, denoted Fig. 1) and levorotatory (right, denoted Fig. 4) tartaric acid. Adapted from Sevin (2015).

living matter; see Goldanskii & Kuz'min (1989). Particularly important is Pasteur's discovery of 1857 that certain unidentified microorganisms had a considerable preference consuming (+)-tartaric acid over (−)-tartaric acid; see the review articles by Gal (2008) and especially Sevin (2015). The connection between a preferred handedness of biomolecules and living matter was reinforced in a number of subsequent papers. The first important one was by Frank (1953), who started his paper by saying "I am informed by my colleague Professor W. Moore that there is still widely believed to be a problem of explaining the original asymmetric synthesis giving rise to the general optical activity of the chemical substances of living matter." He then proposed a model, which contained two key ingredients for producing a systematic handedness: autocatalysis and mutual antagonism. Autocatalysis means making more of itself. This is of course a governing principle of biology, but it is meant here to be used at the molecular level during polymerization, i.e., when long chains of shorter monomers are being assembled into a long macromolecule. When each building block of the polymer has the same chirality, one says that it is isotactic. Mutual antagonism, on the other hand, can be interpreted as the tendency for a monomer of the wrong handedness to spoil the polymerization, so that the polymer would no longer be isotactic.

The basic principle discovered by Frank has been governing many of the ideas reflected in subsequent work in the field of homochirality. One such example was the work of Fajszi & Czégé (1981), who also proposed a mathematical model closely related to that of Frank. However, there are various other clues to the question of homochirality on Earth. One is that there is handedness in one of the four basic forces in nature, the weak force. We explain the details below, but this discovery implies that certain properties of a chiral molecule, for example the dissociation energy, can be different for the two enantiomers. The energy difference is usually a *very* small fraction – below 10^{-10} of the energy of the molecule itself; see Bonner (2000) for a review. Because of the smallness, it is not obvious that this alone can be re-
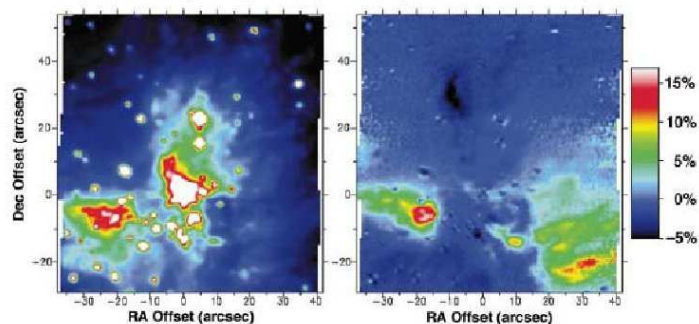
Fig. 4.4 Circular polarization measurements of the star-forming region OMC-1 in the Orion constellation. Note that the circular polarization is predominantly positive in the bulk of the molecular cloud. Courtesy of Bailey et al. (1998).

sponsible for achieving full homochirality. Thus, it is generally believed that some amplification mechanism is always needed.

An interesting astrobiological connection emerges when considering circularly polarized light from astrophysical sources. This is light where the polarization plane rotates with time or position. Star-forming regions in the Orion constellation have been found to emit circularly polarized light preferentially in only one of two possible senses; see Bailey et al. (1998); Bailey (2001); see Figure 4.4 for an image of circular polarization in the Orion molecular cloud (OMC). This is interesting because different enantiomers can dissociate or degrade differently under the influence of circularly polarized light. There is further support for this line of thought in that the chirality of amino acids in space, for example in meteorites, is found to show a slight preference for the levorotatory ones.

We mentioned already that the connection between chirality and the origin of life goes back to an early suggestion by Pasteur. Another connection to astrobiology arises when considering origins of life on other worlds. We will return to this at the end when we discuss possible ways of assessing the reality of extinct or extant life on Mars.

4.2 Enantiomeric cross inhibition: the need for homochirality

We mentioned already that the connection between the origin of homochirality and the origin of life has been suspected since the early work of Pasteur. This connection became more concrete with an important discovery of Joyce et al. (1984). He performed experiments with polynucleotide tem-
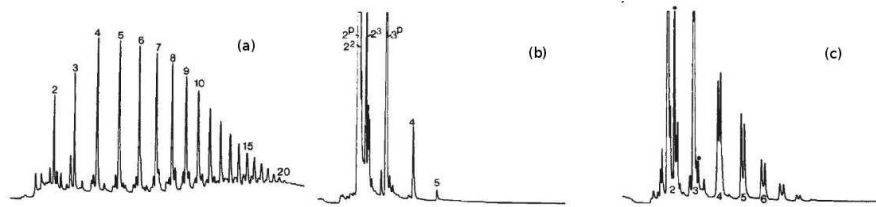
Fig. 4.5 Chromatograms from the work of Joyce et al. (1984) showing template-directed polycondensation of oligo(G_d) on poly(C_d) templates with D mononucleotide (left panel), L mononucleotide (middle panel), and a racemic mixture of D and L mononucleotide (right panel).

plates, which facilitate polymerization with the complementary monomers of the same handedness.[2]

It was thought that polynucleotide templates of one handedness would direct the pairing with monomers of the same handedness and therefore favor the selection of nucleotides of the same chirality. Joyce et al. (1984) performed experiments with polymers of dextrorotatory (D) cytosine (C) nucleobases, poly(C_D), that are expected to pair with guanosine (G) mono-nucleotides to form short strands, oligo(G_D), along the poly(C_D). This was indeed the case and led to the formation of up to 20 base pairs if the solution contained only monomers that are also dextrorotatory; see Figure 4.5a. By contrast, when the solution contained only levorotatory monomers, no polycondensation occurred; see Figure 4.5b.

This was also expected, because base pairs with opposite handedness do not fit together. The surprise came when using a racemic mixture of D and L mono-nucleotides. A racemic mixture would indeed be expected under prebiotic conditions. However, in that case there was no significant polycondensation—not even with the D mononucleotides; see Figure 4.5c. Thus, the idea of using template-directed polycondensation to select only one of two handednesses did not work out. This phenomenon, which is known as enantiomeric cross inhibition, turned therefore out to be a major problem for the RNA world (Gilbert, 1986), unless there was a reason to expect that only monomers of one handedness would be around. Joyce et al. (1984) wrote that "this inhibition raises an important problem for many theories of the origin of life". Bonner (1991) credited Gol'danskii and Kuz'min in saying "that a biogenic scenario for the origin of chiral purity was not viable even in principle, since without preexisting chiral purity the selfreplication characteristic of living matter could not occur." This is where the discovery of the weak force comes into play. It provides a reason why one particular handedness might be preferred. This will be discussed next.

---

[2] Instead of polymerization, one sometimes talks about polycondensation to emphasize the fact that polymerization implies the removal of water in the reaction.
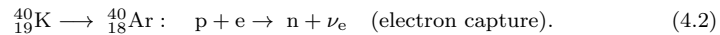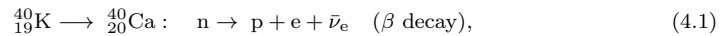
Fig. 4.6 Illustration of lepton helicity. The momentum $\boldsymbol{p}$ is a polar vector, while the spin $\boldsymbol{S}$ is an axial vector, so their dot product is a pseudoscalar, so it changes its sign when inspected in a mirror. The electron from the beta decay of a neutron has $\boldsymbol{p} \cdot \boldsymbol{S} < 0$ and is referred to as *left-handed*.

4.3 The weak force: non-mirrorsymmetry in nature

At the atomic level, there is the strong and the weak force. They are two of the four fundamental forces in nature: gravity, the electromagnetic force, the weak force, and the strong force; see the early review by Ulbricht (1975) in the astrobiological context. The weak force is still rather strong compared with gravity (10^{24} times stronger than gravity), but weak compared with the electromagnetic force (10^{11} times weaker). The weak force is responsible for the decay of free neutrons, whose half-time is only about 10 minutes. The neutron (n) decays then into a proton (p) and an electron (e). This, as well as the reverse process (electron capture), occur also in the nuclei of atoms, for example in the decay of radioactive potassium-40 into calcium-40 and argon-40, where the half-time is 1.25 Gyr. While there is significant astrobiological significance in this, for example for dating rocks,[3] we are here concerned with the fact that the electrons from the decay of neutrons are always left-handed. This means that the spin of the electron is anti-aligned with its momentum; see Figure 4.6. At low energies, however, the spin can flip relative to the momentum, so the handedness of electrons is predominantly a high energy phenomenon.

The fact that electrons produced by β decay are chiral is remarkable, because it means that our physical world is, at least in some respects, different from its mirror image. This goes back to a remarkable discovery by Lee & Yang (1956), which earned them the Nobel Prize in Physics of 1957 "for their penetrating investigation of the so-called parity laws which has led to important discoveries regarding the elementary particles."

---

[3] Measuring the argon inclusions in solidified rocks is the basis for determining the age of rocks. The potassium-40 isotope constitutes only 0.01% of naturally occurring potassium. Its half-time is 1.25 Gyr, making it ideal for geochronology. The two decay reactions are

$$^{40}_{19}\text{K} \longrightarrow {}^{40}_{20}\text{Ca}: \quad \text{n} \rightarrow \text{p} + \text{e} + \bar{\nu}_{\text{e}} \quad (\beta \text{ decay}), \tag{4.1}$$

$$^{40}_{19}\text{K} \longrightarrow {}^{40}_{18}\text{Ar}: \quad \text{p} + \text{e} \rightarrow \text{n} + \nu_{\text{e}} \quad (\text{electron capture}). \tag{4.2}$$

The latter reaction is responsible for the argon in the atmospheres of Earth and Mars.

The connection between the chirality of electrons and that of biomolecules is not immediately evident. There are two different ways of establishing a connection between the handedness imposed by the electroweak force and the handedness in the biomolecules. One is through the fact that the bremsstrahlung emission from chiral electrons rotating around magnetic field lines is circularly polarized with a sense of polarization that depends on the chirality of the electrons. This implies that the sense of polarization from bremsstrahlung is always negative and that this radiation destroys preferentially right-handed amino acids through photolysis. This was found by Goldhaber et al. (1957) and McVoy (1957) in back-to-back papers in the Physical Review almost immediately after the influential paper by Lee & Yang (1956). If the idea that circularly polarized light can affect the stability and selection of biomolecules is to make any sense, one should be able to discover polarized light in nature. Interestingly, star-forming regions of OMC-1 in the Orion constellation have indeed been found to emit right-handed circularly polarized light (Bailey et al., 1998), supporting this basic idea; see Bailey (2001) for a discussion of the astrobiological implications. However, the circular polarization observed by Bailey et al. (1998) occurred at near-infrared wavelengths and is not related to the mechanism of Goldhaber et al. (1957) and McVoy (1957), who considered circularly polarized bremsstrahlung. Bailey et al. (1998) argued that the observed circular polarization is caused by Mie scattering of unpolarized light, but this mechanism is unrelated to the weak force. It is therefore conceivable that also left-handed circularly polarized light could have been produced in the opposite direction.

Instead of relying on starlight, there is yet another possibility. Muons, like electrons, belong to the group of fermions that tend to have a certain handedness. Muons are about 200 times more massive than electrons and can therefore be more effective in producing strongly circularly polarized radiation. Muons occur in the cosmic radiation on Earth. They are only produced when an energetic cosmic particle hits the Earth's atmosphere and produces a muon shower. For this reason, the muons in the cosmic radiation can play a significant role in affecting the chirality of biomolecules Globus & Blandford (2020). Unlike the observed circular polarization from the OMC-1 in the Orion constellation, the sense of circular polarization from this mechanism is connected with the weak force and therefore, just like in the case of bremsstrahlung, only one of the two senses are possible, giving rise to the preferential destruction of right-handed amino acids.

There is another completely different connection between biomolecules and the weak force. Quantum-mechanical calculations have shown that the dissociation energies for D and L molecules are slightly different (Hegstrom, 1984; Hegstrom et al., 1980; Mason & Tranter, 1984). Therefore, the D and L amino acids in a racemic mixture will degrade at different rates, which leads to an excess of L amino acids.

4.4 Chiral amino acids in meteorites

Amino acids have been found in some meteorites (Engel & Macko, 1997). Two particular meteorites are often discussed in connection with the enantiomeric excess of amino acids: the Murray and the Murchison meteorites (Pizzarello & Cronin, 2000). Those are carbonaceous chondrites, which means that they are carbon-rich. They are also rich in organics, as was superficially evidenced by the smell reported by initial eyewitnesses of the Murchison meteorite. Interestingly, Table 1.5 of Rothery et al. (2008) lists 18 different amino acids that have been found not only in the Murchison meteorite, but also in the Miller–Urey experiment (Miller, 1953). Twelve of them are not found in proteins on Earth. This is interesting, because it suggests that those amino acids were indeed originally present in the meteorite and could not have come from contamination by life after the meteorite landed on Earth. Those amino acids that are found on Earth include glycine, alanine, valine, proline, aspartic acid, and glutamic acid

The sense of the enantiomeric excess is the same in the two meteorites, corresponding to levorotatory amino acids, but the amount is different (Pizzarello & Cronin, 2000). In addition, there is the possibility that the enantiomeric excess may be caused by terrestrial contamination (Bada, 1995). But, as emphasized above, this would only apply to the six amino acids that are also found on Earth. In particular, those amino acids that have the clearest enantiomeric excess are also those that are most vulnerable to contamination; see Ehrenfreund et al. (2001) for a discussion of terrestrial contaminants in connection with the carbonaceous chondrites Orgueil and Ivuna. They are of the type CI (I for Ivuna) and are extremely fragile and therefore susceptible to terrestrial weathering. In Orgueil, alanine was found to be racemic and was argued to be abiotic in origin (Ehrenfreund et al., 2001). They could not, however, support the suggestion of terrestrial contamination with corresponding soil samples. Incidently, the Orgueil meteorite is also known for a famous contamination hoax; see Anders et al. (1964), who discusses the paper by Cloez (1864) claiming the existence of life on the meteoritic parent body a few weeks after Pasteur's famous lecture to the French Academy on the spontaneous generation of life.

Among the possible causes for the enantiomeric excess of meteoritic amino acids, there is the aforementioned effect of circularly polarized starlight. Circularly polarized ultraviolet light could have preferentially destroyed one of the two chiralities through photolysis (Zeldovich et al., 1977). The experiments of Bonner et al. (1981) with a D L mixture of leucine showed that right-handed circular polarized light leads to a preferential destruction of D leucine, while left-handed circular polarized leads to a preferential destruction of L leucine; see also (Meierhenrich & Thiemann, 2004) for recent experiments. To explain the systematic L excess of amino acids on Earth, one would need the protosolar nebula to be irradiated by right-handed polarized light. Indeed, the star-forming region OMC-1 has been found to emit right-handed
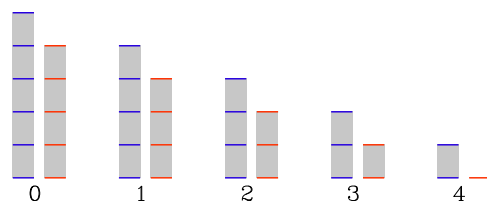
Fig. 4.7 Sketch showing the effect of enantiomeric cross inhibition only. Red and blue bars indicate opposite enantiomers, with the blue one being initially in the majority by one "unit", the separation between subsequent bars. The gray columns indicate the total amounts, which is 5 units for the column with blue bars and 4 units for the column with red bars. In the end, in step 4, only one unit of the enantiomer marked with blue bars survives.

circularly polarized light, supporting this basic idea (Bailey et al., 1998; Bailey, 2001; Boyd et al., 2018). However, as discussed above, also left-handed circularly polarized light could have been produced in the opposite direction. Therefore, any systematic L excess of amino acids caused by this mechanism would have been by chance.

The enantiomeric excess found in some amino acids is at most around 1–2%. This would be too small to avoid the problem reported by Joyce et al. (1984). So, even if there is an external effect producing a systematic enantiomeric excess, we always need an amplification mechanism. Therefore, we discuss next the Frank mechanism and move then to some variants of it that avoid either autocatalysis or enantiomeric cross inhibition. We begin by explaining first the basic idea.

4.5 The basic idea behind the Frank mechanism

The essence of the mechanism of Frank (1953) is the *combination* of two ingredients operating in a substrate: catalysis of molecules for their own production and "anticatalysis" that corresponds to some antagonism or deleterious effect. He even talks about "poisoning" one of the two enantiomers out of existence. In fact, he called his simple mathematical model a "life model", suggesting already back then that he was thinking of them as being processes acting at the moment when the first life emerged.

The essence of Frank's model is perhaps best explained graphically. For this purpose, it is most instructive to begin with the deleterious effect by assuming that an equal amount of D and L enantiomers eliminate each other in each reaction step. This is illustrated in Figure 4.7, where we indicate the amount of D enantiomers with blue bars and the amount of L enantiomers with red bars.
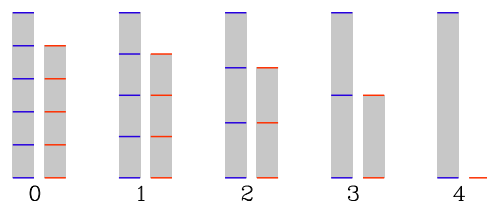
Fig. 4.8 Similar to Figure 4.7, but in each reaction step, the separations between subsequent bars has been stretched by a certain factor such that the column with the blue bars retains the same height. The stretching emulates the effect of autocatalysis. In the end, again only the enantiomers marked with blue bars survive, but now, because of the stretching, the amount is no longer small.

We see that, in the end, only D is left (see the blue bars), but the amount is very small, namely just as big as the initial difference by which one of the two enantiomers exceeded the other. This is why we also need autocatalysis. Autocatalysis is a process that is not enantioselective, i.e., it works the same way for the D and L enantiomers. This is demonstrated by stretching out the columns by a factor such that the highest column always retains the original height; see Figure 4.8. It is instructive to quantify here the enantiomeric excess (e.e.) as the ratio of the difference to the sum of the concentrations of right- and left-handed compounds, i.e.,

$$\text{e.e.} = \frac{[D] - [L]}{[D] + [L]} \tag{4.3}$$

At each each, the value of e.e. in Figs. 4.7 and 4.8 is the same: $1/(5+4) = 1/9$ initially, then $1/(4+3) = 1/7$, $1/(3+2) = 1/5$, $1/(2+1) = 1/3$, and finally $1/1 = 1$.

Frank's paper was mathematical, which may have been a reason why it was not widely recognized in the biology community at the time. In fact, it was not quoted in the work of Joyce et al. (1984), who discovered enantiomeric cross inhibition in the context of nucleotides. It was only with the paper of Sandars (2003) that Frank's mutual antagonism was identified with enantiomeric cross inhibition. It was clear from Frank's work that, as long as both reactions, autocatalysis and antagonism, remain active, the racemic state is unstable and there will be a bifurcation into a chiral state with an excess of either D or L enantiomers; see also Sandars (2005), where enantiomeric cross inhibition was no longer regarded as a problem, but as an essential ingredient in achieving full homochirality.

In the Frank mechanism, there must be at least a very small initial imbalance which will then be amplified. However, this is not a problem because, even if we tried to construct a purely racemic mixture in the laboratory, there will always remain a tiny imbalance. This is just for the same reasons that
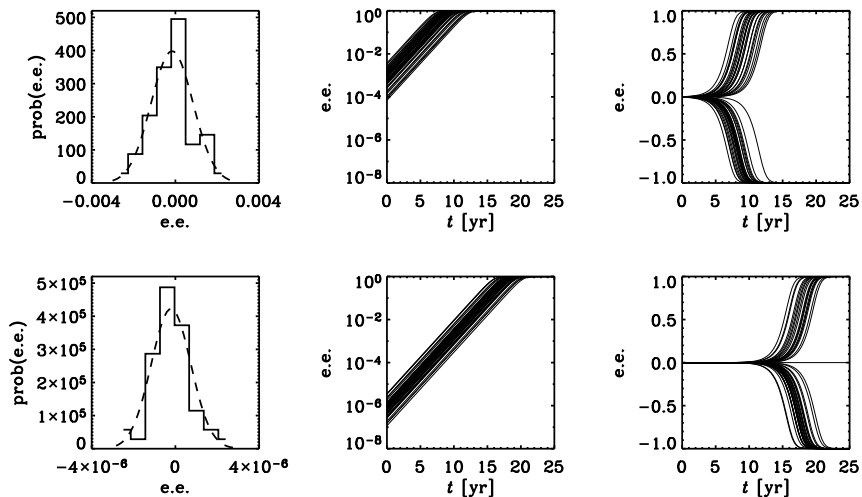
Fig. 4.9 Probability distribution of the initial enantiomeric excess (e.e.) for racemic mixtures with 10^6 and 10^{12} molecules together with the resulting evolution of e.e., both in logarithmic and linear representations. The dashed lines give a gaussian fit to the distribution function. Adapted from Brandenburg et al. (2007).

in a cup of blueberries we will hardly ever have exactly the same number twice.[4]

Given that the racemic state is unstable, the enantiomeric excess, as defined in Eq. (4.3), will grow exponentially in time and it does therefore not matter how small the initial imbalance in the concentrations of D and L was. To demonstrate this more clearly, we use here a figure of Brandenburg et al. (2007), who considered the model of Plasson et al. (2004), which we discuss later in more detail in Section 4.10. This model also has the property that the racemic state is unstable and that the system evolves toward one of the two homochiral states.

In the following, we discuss an ensemble of solutions of the model of Plasson et al. (2004) with different realizations or initial states, which consisted of a racemic mixture of equally many D and L enantiomers. Figure 4.9 shows that one always obtains a fully homochiral state, but in about 50% of the cases (or in 50% of the realizations of the same experiment), one obtains eventually

---

[4] If you take a cup of blueberries, for example, the exact number varies between 65 and 70 (`https://www.howmuchisin.com/produce_converters/blueberries`), so we must always expect there to be a small imbalance in the number if we say we have an equal *amount* of D and L enantiomers. Mathematically, this imbalance grows with the square root of the number of molecules (or blueberries) and would be about $\pm 10^{12}$ for one mole with $\mathcal{N} = 6 \times 10^{23}$ molecules (or ± 8 for 65 blueberries); the fractional imbalance is $1/\sqrt{\mathcal{N}} = 10^{-12}$ in one mole (or 12% for 65 blueberries).

a state with either just D enantiomers, and in the other 50% of the cases or realizations, one with only L enantiomers. When we talk about different cases or realizations, we must realize that the genesis of life on Earth is just one such realization. Another one may have occurred on Mars, or in the atmosphere of Venus, or elsewhere in the Galaxy. Of course, there is also the possibility of multiple geneses on Earth alone, with certain lifeforms being either completely or partially wiped out (Davies & Lineweaver, 2005). The latter case may be particularly interesting in models where we allow for chemical evolution in models with spatial extent, which will also be discussed later in Section 4.9.

4.6 Evidence for autocatalysis

Unlike the process of enantiomeric cross inhibition, where we have referred to the experiments of Joyce et al. (1984), the actual evidence for autocatalysis is poor. In fact, there is only the classical reaction of Soai et al. (1995) that exhibits autocatalysis and can lead to a finite enantiomeric excess; see Gehring et al. (2010) and Athavale et al. (2020) for more recent work clarifying the implications of the Soai reaction. However, the basic idea of autocatalysis remains plausible, especially since the discovery by Guerrier-Takada & Altman (1984) and Cech (1986) that RNA molecules can exhibit autocatalytic functionality. This was a very important discovery that earned Sidney Altman and Thomas R. Cech the Nobel Prize in Chemistry in 1989 "for their discovery of catalytic properties of RNA." It is this mechanism that is at the heart of the idea of an RNA world (Gilbert, 1986).

It is important to realize that the existing evidence for autocatalysis is irrelevant from an astrobiological viewpoint. This is particularly clear in view of the fact that the Soai reaction requires zinc alkoxides as an additional crucial catalyst. Those compounds are not generally believed to play a role on the early Earth.

Autocatalysis in the sense of making more of itself is obviously a basic principle of life, but this is already at a rather complex and not at the level of individual molecules. It is therefore possible that autocatalysis does not play a significant role and that it is rather the process of network catalysis (Plasson, 2015), i.e., the combined action of different molecules that lead to the desired appearance of what is in the end equivalent to autocatalysis. We will return to this in Section 4.10, when we discuss a particular sequence of reactions that, in the end, have the effect of autocatalysis, even though autocatalysis is not present in any individual reaction.
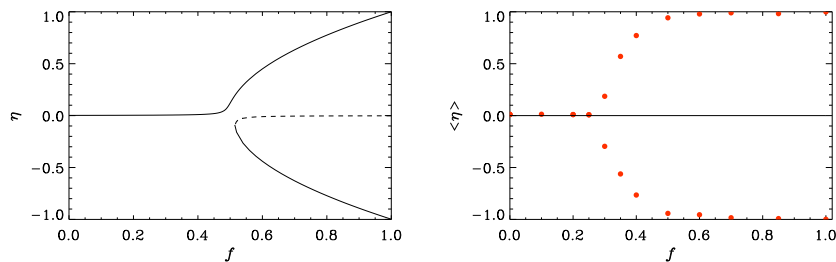
Fig. 4.10 Bifurcation diagrams showing a slight preference for positive enantiomeric excess (e.e., here denoted by η). The left panel has been adapted from Brandenburg et al. (2005), where the bifurcation begins for a fidelity f that is clearly below the otherwise critical value of $f = 0.5$. (The dashed line denotes the unstable solution.) The right panel has been adapted from Brandenburg (2019), who considered a stochastic model where $f = 0.2$ was assumed.

4.7 The effect of an external chiral influence

In the beginning of this review, we have discussed extensively the possibility of a systematic bias resulting eventually from the fact that the weak force introduces a preference of one of two handednesses through one or several possible effects. Those would always favor L amino acids and D sugars. On the other hand, we have now seen that the Frank mechanism can result in full homochirality of either chirality. Does this mean that the bias introduced by the weak force is unimportant? Maybe not quite. It depends on how strong the external influence is in comparison with the speed of autocatalysis, which determines the rate of the instability. This was first discussed in the work of Kondepudi & Nelson (1983, 1985) in papers that appeared just at the time as that of Joyce et al. (1984), but, at the time, neither of those authors mentioned the work of Frank.

The paper by Kondepudi & Nelson (1983, 1985) was in principle quite general and therefore applicable to other symmetry breaking instabilities. In essence, the effect of the bias is that it makes the bifurcation asymmetric. A symmetric bifurcation is one where the enantiomeric excess (positive or negative) departs away from strictly zero as some bifurcation parameter increases. Sandars (2003) identified this bifurcation parameter with the fidelity of the autocatalytic process, which measures the probability with which the catalytic process does indeed facilitate the polymerization with monomers of the same chirality instead of the opposite one. The fidelity f is unity (zero) when the autocatalytic process always (never) produces polymerization with the same handedness.

In Figure 4.10 we show a bifurcation diagram from the work of Brandenburg et al. (2005), where we see that for all values of the fidelity f, the

solution with positive enantiomeric excess (η) is stable. For $\eta \gtrsim 0.5$, the solution with negative η is also stable, but to reach this solution, the initial fluctuations must be large enough. The complete bifurcation diagram also contains an unstable solution, which corresponds to the watershed between the two stable branches. In the left hand plot of Figure 4.10, it is shown as a dashed line. Similar diagrams have also appeared in the works of Kondepudi & Nelson (1983) and later in the review of Avetisov et al. (1991).

4.8 Polymerization model of Sandars (2003)

Looking at the chromatographs of Joyce et al. (1984), we see that the ultimate goal is to assemble long polymers. For this reason, Sandars (2003) developed a polymerization model for D and L nucleotides, where he also allowed for enantiomeric cross inhibition. In his model, monomers of the D and L forms are being produced at rates, Q_D and Q_L, respectively, that are proportional to same reaction rate k_C and the concentration of some substrate $[S]$, i.e.,

$$Q_D = k_C[S]\left\{\tfrac{1}{2}(1+f)C_D + \tfrac{1}{2}(1-f)C_L + C_{0D}\right\}, \qquad (4.4)$$

$$Q_L = k_C[S]\left\{\tfrac{1}{2}(1+f)C_L + \tfrac{1}{2}(1-f)C_D + C_{0L}\right\}, \qquad (4.5)$$

where $0 \leq f \leq 1$ is the fidelity, C_L and C_D are parameters describing the global handedness of the system [the concentrations of the longest possible chains of left- and right-handed polymers for Sandars (2003) and quantities proportional to the masses of all polymers of the D and L forms for Brandenburg et al. (2005)]. These parameters are introduced in such a way that for $f > 0$ in Eqs. (4.4) and (4.5), Q_D increases with C_D, and Q_L increases with C_L. The parameters C_{0D} and C_{0L} allow for the possibility of non-catalytic production of left- and right-handed monomers. They can be different from zero when there is an external bias or external influence. When $C_{0D} = C_{0L} = 0$, Eqs. (4.4) and (4.5) show that $Q_D = k_C[S]C_D$ and $Q_L = k_C[S]C_L$ when $f = 1$, while $Q_D = Q_L = k_C[S](C_D + C_L)/2$ when $f = 0$.

Sandars (2003) assumed that the catalytic effect depends on the concentrations of the longest possible chains of left and right handed polymers. Brandenburg et al. (2005) adopted a similar model, but assumed that C_D and C_L to be proportional to the masses of all polymers of the D and L forms, respectively. This allowed them to extend the model to much longer polymers without needing to wait for the longest one to appear before autocatalysis became possible at all.

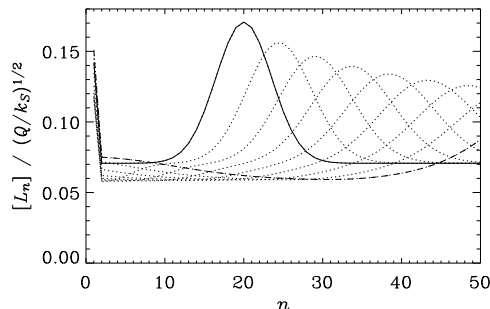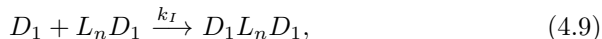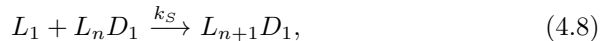The full set of reactions included in the model of Sandars (2003) is (for $n \geq 2$)

Fig. 4.11 Normalized concentration $[L_n]$ versus n showing a wave-like evolution of an initial Gaussian profile (solid line). All later times are shown as dashed lines, except for the last time, which is shown as a long-dashed line. Adapted from Brandenburg et al. (2005).

$$L_n + L_1 \xrightarrow{2k_S} L_{n+1}, \tag{4.6}$$

$$L_n + D_1 \xrightarrow{2k_I} L_nD_1, \tag{4.7}$$

$$L_1 + L_nD_1 \xrightarrow{k_S} L_{n+1}D_1, \tag{4.8}$$

$$D_1 + L_nD_1 \xrightarrow{k_I} D_1L_nD_1, \tag{4.9}$$

where k_S and k_I are suitably chosen reaction rates for symmetric autocatalysis and (non-symmetric) inhibition, respectively. For all four equations we have the complementary reactions obtained by exchanging $L \rightleftarrows D$. The polymerization starts from a large but limited set of monomers that all begin to develop longer polymers. Because the number of monomers was limited, the theoretically obtained chromatograms show a characteristic wave-like motion with increasing time; see Figure 4.11.

Particularly important is of course the case where monomers of both chiralities exist. In that case, the result depends on the fidelity of the autocatalytic reactions; see Figure 4.12 for such a result. We see that longer polymers can only be produced when the fidelity is relatively high. The lack of sufficient fidelity therefore explains the limited length of polymers found in the work of Joyce et al. (1984).

4.9 Spatiotemporal chirality dynamics

In all the chemical reactions discussed so far, the assumption was made that the system is well mixed. This means that the concentrations $[D_n]$, $[D_nL]$, etc, are the same everywhere. On larger length scales, this assumption must
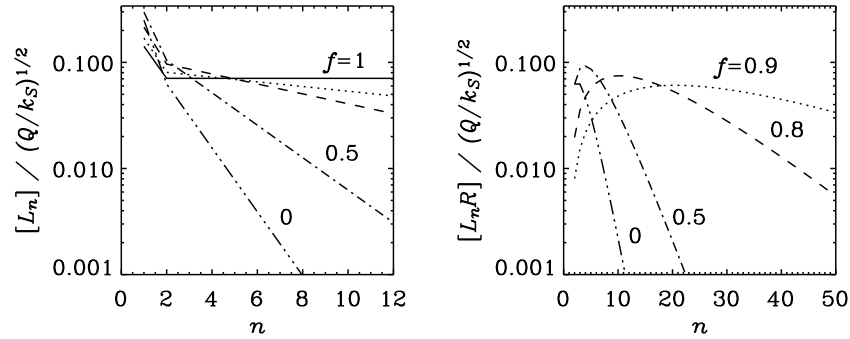
Fig. 4.12 $[L_n]$ (left) and $[L_nD]$ (right) of equilibrium solutions for different values of f. For $f = 1$ we have $[L_nD] = 0$, which cannot be seen in the logarithmic representation. Adapted from Brandenburg et al. (2005).

eventually break down. Even on the scale of alkaline hydrothermal vents, where many scientists place the origin of life (Russell, 2006) the relevant chemical reactions would take place within small semiporous cells. It is then conceivable that similar reactions take place in neighboring compartments that would be formed by the sulfurous precipitants from these vents. Russell (2006) draws here an analysis to the chemical gardens that would allow for a growing arrangement of new compartments, which could act as primitive cells and would, in principle, allow for Darwinian evolution as these chemical reactions propagate from one layer of compartments to the next; see also Russell et al. (2014) and Barge et al. (2017, 2019) for more recent developments. In each of these compartments, strong spatial gradients and 10^8-fold concentration enhancements can be achieved through thermal convective flows when the aspect ratio of the compartment is sufficiently large (Baaske et al., 2007). This setup can also lead to oscillations, which can locally lead to exponential replication of nuclei acids, analogous to the polymerase chain reaction (Braun & Libchaber, 2002).

In the scenario described above, we can no longer talk about a well mixed system. Therefore, the concentrations must be regarded as function not only of time, but also of space. Because the chemistry in neighboring compartments is loosely coupled by diffusion terms, there would be spatio-temporal evolution. In that case, the chemical reaction equations attain a spatial diffusion term. The resulting system of equations is usually referred to as reaction–diffusion equations. Such models, but for only one instead of several species, have frequently been employed in modeling the dynamics of diseases such as the black death (Noble, 1974) or rabies (Källén et al., 1985; Murray et al., 1986). It has also been used to model the spreading of the novel coronavirus,
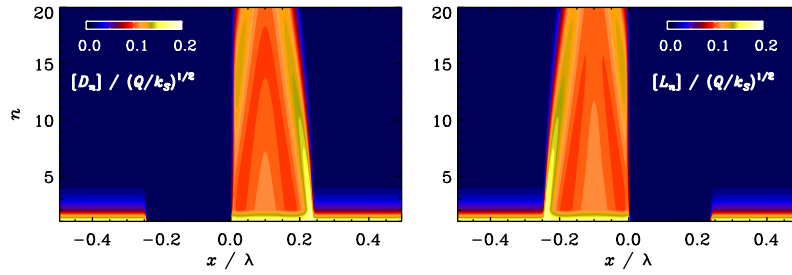
Fig. 4.13 Color scale plots of $[D_n]$ and $[L_n]$ after 0.8 diffusion times as a function of position x and polymer length n. In $0 < x/\lambda < 0.25$, only D polymers exist (left) and no L polymers at all (right), while in $-0.25 < x/\lambda < 0$ it is the other way around. Adapted from Brandenburg & Multamäki (2004).

where the total number of cases was found to follow a quadratic or piecewise quadratic growth behavior (Brandenburg, 2020).

To address the question of homochirality in an extended system, Brandenburg & Multamäki (2004) employed a similar approach, but with two or multiple species. Multiple species occur when we invoke polymers of different length and composition of different species for the D and L forms. They found that a given species tends to spread through front propagation. It turned out that, once two populations of opposite chirality meet, the front can no longer propagate and the evolution comes to a halt. This result was first obtained in a one-dimensional model, where the concentrations of D and L depend on just one spatial coordinate x and on time t. The result is shown in Figure 4.13, for the evolution of short polymers. These are all regarded as separate species. The initial condition consists of a small number of monomers of the L form at one position (at $x/\lambda = -0.1$ in Figure 4.13, where λ is the length of the domain) and a three times larger number of monomers of the D form at another position (at $x/\lambda = +0.1$). The theoretical chromatograms are stacked next to each other for each x position. We see that in both positions, longer polymers are produced, indicated by the yellow-reddish colors. The initially threefold larger number of D monomers is insignificant, because the growth is exponentially fast soon saturates at the same level as that for the L monomers, when the polymers have reached their maximum size. At the same time, polymers of the same handedness can still be produced by diffusion to the neighboring positions. This leads to a propagation front. However, when polymers of opposite chirality emerge at neighboring positions, the front stops (here at $x \approx 0$), while on the other two sides, the reaction fronts still diffuse further outward.

More interesting dynamics is possible when the system is two-dimensional, corresponding to different locations on the Earth's surface. In that case, the fronts between regions with monomers and polymers of opposite handedness can be curved. It turned out that then the fronts are never precisely straight
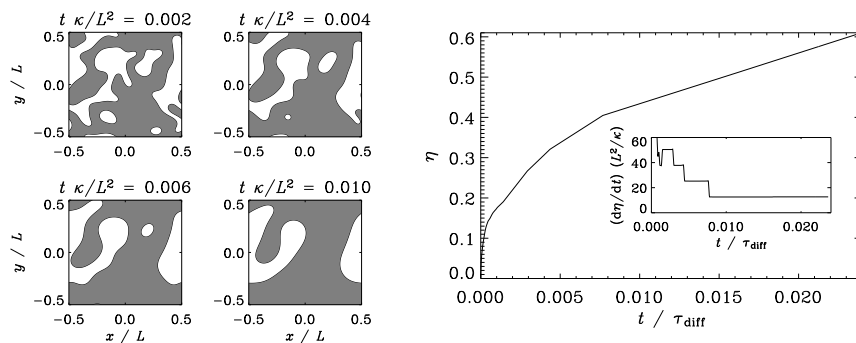
Fig. 4.14 *Left*: Fractional concentration of one chirality versus position (x and y) at four different times t, normalized by the diffusivity κ per total surface area λ^2, so $t\kappa/\lambda^2$ is nondimensional. In this numerical simulation, $\kappa/(\lambda^2\lambda_0) = 2 \times 10^{-4}$, and the resolution was 1024^2 mesh points. The number of disconnected regions decreases from 4 in the first plot to 3, 2, and 1. *Right*: Evolution of enantiomeric excess η for the model shown in the left. The inset shows the normalized slope. Note the four distinct regimes with progressively decreasing slope. Adapted from Brandenburg & Multamäki (2004).

and can therefore still propagate. Interestingly, the propagation is always in the direction of maximum curvature. This result has also been obtained by Gleiser & Walker (2012). This then implies that a closed circular front will always shrink and never expand; see left Figure 4.14. The speed of shrinking depends just on the number of individual closed fronts. Each time a closed front merges with another one to form a single one, the speed decreases; see the right panel of Figure 4.14. In particular, this means that, even if, say, the L enantiomers were initially in the majority, but in such a way that they would be enclosed in an island surrounded by enantiomers of the opposite handedness, the enantiomeric excess would develop toward the handedness that was present on the periphery of the domain; see Figure 4.15 for such an illustration with the model of Plasson et al. (2004).

The reason for this particular propagation direction is quite simple. Imagine that we place D and L molecules around a circular front, then the number of molecules on the inner front is would be one less than the number of molecules on the outer front; see Figure 4.16 for an illustration.[5]

---

[5] To understand why the difference in the number of molecules between the outer and inner circles is always just three, let us imagine the molecules being represented by little discs of radius r on the periphery of a circle of radius R. The circumferences of the outer and inner peripheries are $2\pi(R\pm r) = 2\pi R \pm \pi r$ for the upper and lower signs, respectively. The difference is therefore $2\pi r \approx 3d$, where $d = 2r$ is the diameter of each disc. The difference in the number of discs is there for three.
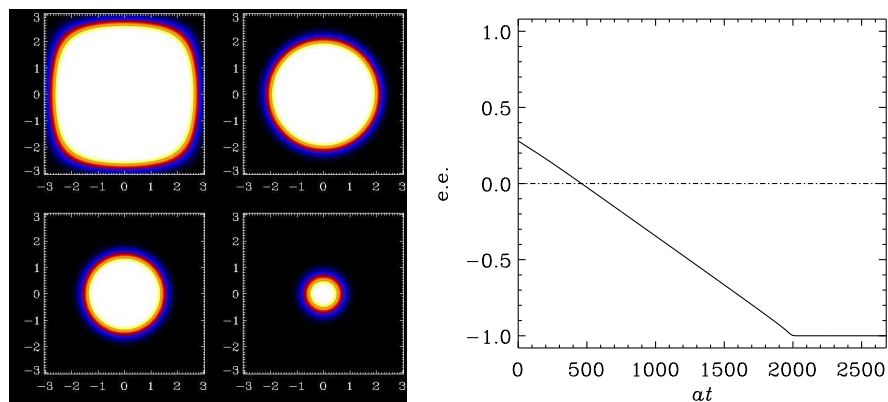
Fig. 4.15 *Left*: Shrinking of an initially large patch of molecules of the D form surrounded by molecules of the L form. *Right*: The resulting enantiomeric excess (e.e.) versus time t, scaled with the activation rate a, so at is nondimensional. Note that it was initially positive, but reaches later complete homochirality with $\eta = -1$.
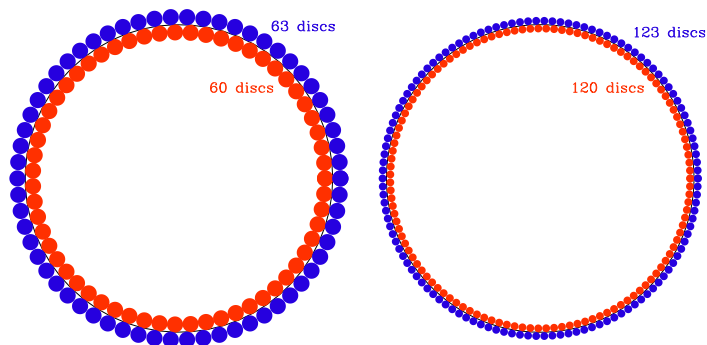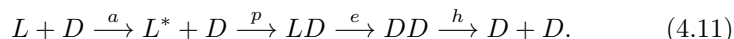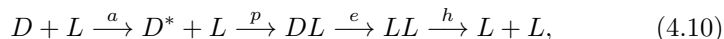

Fig. 4.16 Sketch illustrating that densely packed discs inside the periphery of a circle differ in their number from those outside the periphery by just 3. This result is independent of the total number; compare the left and right illustrations with 60 and 120 discs, respectively. As time goes on, pairs of red and blue discs get eliminated and the circle shrinks, because the number of discs inside the periphery is slightly smaller (by three) than the number of discs outside the periphery. The smallness of the difference in the numbers on the inner and outer peripheries is the reason for the shrinking of the circle slowing down.

4.10 Recycling Frank: the peptide model of Plasson et al.

We said already in Section 4.6 that autocatalysis may not be a particularly evident process on the early Earth. For that reason, Plasson et al. (2004) devised a completely different mechanism that they advertised as "recycling

Frank". It is based on the combination of the following four important reactions: activation (A), polymerization (P), epimerization (E), and depolymerization (D). So the resulting model is also referred to as the APED model. A variant of this model was studied by Konstantinov & Konstantinova (2018).

It is important to emphasize that there is no explicit autocatalytic reaction. However, the combined sequence of reactions (Brandenburg et al., 2007)

$$D + L \xrightarrow{a} D^* + L \xrightarrow{p} DL \xrightarrow{e} LL \xrightarrow{h} L + L, \tag{4.10}$$

$$L + D \xrightarrow{a} L^* + D \xrightarrow{p} LD \xrightarrow{e} DD \xrightarrow{h} D + D. \tag{4.11}$$
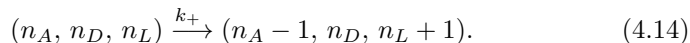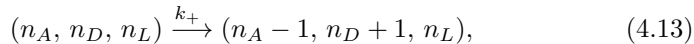
does effectively result in an autocatalytic reaction, but it is not a direct one. First of all, it requires an activation step, indicated by asterisk, a polymerization step (with the rate constant p), an epimerization step (with the rate constant e), and finally a depolymerization step (with the rate constant h). Because the autocatalysis in indirect, this sequence of steps can therefore be regarded as a simple example of a network catalysis (Plasson, 2015; Hochberg et al., 2017).

4.11 Fluctuations instead of autocatalysis or enantiomeric cross-inhibition

During the last decade, there has been some increased interest in the role of fluctuations; see a recent review by Walker (2017). Fluctuations can play important roles in diluted systems, in which the number of molecules is small. In such case, rate equations no longer provide a suitable description of the relevant kinetics when the system is dilute and reactions are rare (Gillespie, 1977; Toxvaerd, 2014). In that case, a stochastic approach must be adopted. This may be relevant to the work of Toxvaerd (2013), where homochirality has been found without apparent autocatalysis or enantiomeric cross-inhibition. Instead of solving rate equations, as discussed in the previous sections, one solves stochastic equations. This means that at each reaction step, the state of the system changes, but with a reaction that is taken to depend on chance with a certain probability. The system is then described by vector $\boldsymbol{q} = (n_A, n_D, n_L)$, where n_A denotes the numbers of achiral molecules and n_D and n_L denotes the number of molecules of the D and L forms, respectively. In the model of Brandenburg (2019), seven different reactions were considered, each with a certain probability. Not all those seven reactions need to be possible in a certain experiment, so the probability for some reactions can be zero. Applying a single reaction step with enantiomeric cross inhibition implies

$$(n_A, n_D, n_L) \xrightarrow{k_\times} (n_A + 2, n_D - 1, n_L - 1), \tag{4.12}$$
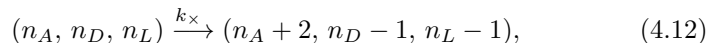
i.e., the numbers of D and L get reduced by one, and that of A increases by two. We can also include spontaneous deracemization reactions, i.e.,

$$(n_A, n_D, n_L) \xrightarrow{k_+} (n_A - 1, n_D + 1, n_L), \tag{4.13}$$

$$(n_A, n_D, n_L) \xrightarrow{k_+} (n_A - 1, n_D, n_L + 1). \tag{4.14}$$

To model different reaction rates, the different reactions must happen with different probabilities. This is done by taking at each reaction step a random number between zero and one. Suppose we want to model enantiomeric cross inhibition together with spontaneous deracemization, then the probability that the first reaction happens is proportional to $k_\times$, and the probability that one of the other two reactions in Eqs. (4.14) and (4.14) occurs is proportional to $k_+/2$. If we also allow for the possibility that nothing happens (probability proportional to k_0), then our scheme with $\boldsymbol{q} \to \boldsymbol{q} + \Delta\boldsymbol{q}$ is as follows:

$$\text{if} \quad 0 \leq r < r_1 \equiv k_\times \qquad\qquad \text{then } \Delta\boldsymbol{q} = (2, -1, -1), \tag{4.15}$$

$$\text{if} \quad r_1 \leq r < r_2 \equiv r_1 + k_+/2 \qquad \text{then } \Delta\boldsymbol{q} = (-1, 1, 0), \tag{4.16}$$

$$\text{if} \quad r_2 \leq r < r_3 \equiv r_2 + k_+/2 \qquad \text{then } \Delta\boldsymbol{q} = (-1, 0, 1), \tag{4.17}$$

$$\text{if} \quad r_3 \leq r < 1 \qquad\qquad\qquad \text{then } \Delta\boldsymbol{q} = \boldsymbol{0} \text{ (no reaction)}. \tag{4.18}$$

Note that $k_\times + k_+ + k_0 = 1$ is here assumed. This particular experiment was referred to as experiment III in Brandenburg (2019), where $k_0 = 0$ was assumed. As he varied $k_\times$, k_+ was assumed to vary correspondingly such that $k_+ = 1 - k_\times$. The results of this experiment are similar to those with spontaneous deracemization replaced by autocatalysis, which is referred to as experiment I in Figure 4.17. Here, the autocatalysis rate is varied such that $k_C = 1 - k_\times$. This is the standard Frank model, but for a diluted system, while model III is close to that of Sugimori et al. (2008, 2009), who were the first to find a transition to full homochirality even without autocatalysis. Next, in experiment II, there is autocatalysis, but no enantiomeric cross inhibition and just spontaneous racemization instead. This type of model was first considered by Jafarpour et al. (2015, 2017). The transition to full homochirality was originally though impossible in such a model (Stich et al., 2016).

In a comparative study, all these processes were studied within a single unified model. In Figure 4.17 we show the results of the four different experiments. We mentioned already experiments I–III. In experiment IV, by comparison, there is just racemization and deracemization, but neither autocatalysis nor enantiomeric cross inhibition. In that case, the average of the modulus of the enantiomeric excess, $\langle|\eta|\rangle$, no longer reaches unity, but levels off at about 0.5 when $k_+ \gtrsim 0.4$. We also see from the red lines that the achiral compounds (A) get depleted in favor of producing chiral ones either of the D or the L form.
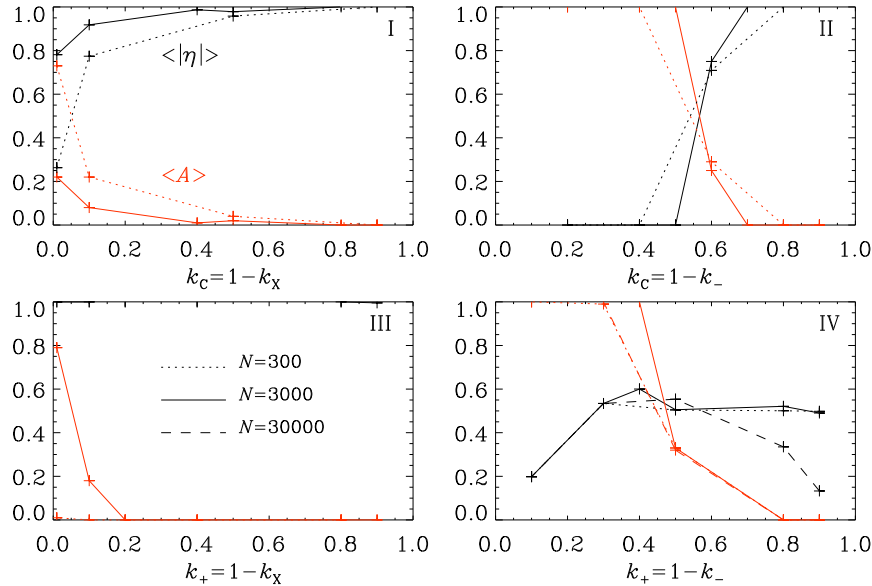
Fig. 4.17 Bifurcation diagrams of $\langle|\eta|\rangle$ (black) and $\langle A\rangle$ (red) for $N = 3000$ (solid lines) and $N = 300$ (dotted lines) as a function of parameters for models I, II, III, and IV. Adapted from Brandenburg (2019).

4.12 Chirality from a Martian Labeled Release experiment

Back in 1976, when the Viking I and II landers visited the Chryse Planitia and Utopia Planitia regions, respectively, many of the things we now know about Mars were still unclear. In particular, the existence of water on Mars was still very much an open question. Nevertheless, one was relatively optimistic at the time. Both landers came with advanced experiments on board to look for life. One of the experiments, the Labeled Release (LR) experiment, was actually successful (Levin & Straat, 1976, 1977), but another experiment never detected any organics, which was decisive enough to conclude that no life was detected after all (Klein et al., 1976).

The idea behind the LR experiment is simple: take Martian soil, mix it with water and organics as nutrients, and see whether a metabolic reaction occurs that decomposes the nutrients and produces a gaseous waste product, for example methane or carbon dioxide; see the recent account by Levin & Straat (2016), where detailed tests with various terrestrial soils were presented. The carbon atoms of the nutrients were labelled with carbon-14 isotopes, a technique commonly used in medicine, which allows one to trace those labeled carbon atoms by their radioactivity. To identify the gaseous waste product,

one simply measured the level of radioactivity. Control experiments with sterilized soil showed that only fresh Martian soil produced a reaction. The Viking laboratories were flexible enough to perform additional experiments with lower sterilization temperatures. The critical temperature below which no sterilization occurred was found to be around $50°$. Those temperatures would appear reasonable for Martian cryophiles, but are generally too low for sterilization on Earth. The experiment was tested in various deserts on Earth and it was able to detect metabolism at measurable levels.

It is only since 2012 that organics were detected on the Martian surface by the Curiosity rover; see Voosen (2018) for a popular account. We also know that organics get quickly destroyed by perchlorates, in particular $KClO_4$, which were discovered on the Martian surface by the Phoenix lander in 2008 (Hecht et al., 2009). Such processes could potentially result in reactions found with the LR experiment (Quinn et al., 2005), but it remains puzzling why a critical sterilization temperature of $50°$ was found, and not much higher, for example. Thus, while an explanation in terms of abiotic processes has not been fully conclusive (Valdivia-Silva, 2012), the explanation that life was actually detected might seem more straightforward (Levin & Straat, 2016). However, as already noted by Carl Sagan, "the more extraordinary the claim, the more extraordinarily well-tested the evidence must be. The person making the extraordinary claim has the burden of proving to the experts at large that his or her belief has more validity than the one almost everyone else accepts." In any case, it seems justified to repeat this experiment to clarify the phenomenon that the Viking landers discovered back in 1976; see also the recent paper by Carrier et al. (2020).

Given that the experiment is relatively simple and can detect life under harsh conditions on Earth, it would be interesting to repeat some variants of it in the future. One such variant would be to allow for the detection of handedness. This would constitute a more conclusive signature of life than just the discovery of some metabolism. Such an experiment can be done by using chiral nutrients, which goes back to the old findings of Pasteur of 1857 that certain microorganisms had a preference for consuming (+)-tartaric acid over (−)-tartaric acid; see the reviews by Gal (2008) and Sevin (2015).

In Figure 4.18 we show the result of recent experiments by Sun et al. (2009) using different types of eukarya, bacteria, and archaea, which were given either D sugars or L sugars. In most of the cases there was a clear preference in the microbes taking up the naturally occurring D sugars compared with the synthetically produced L sugars. Subsequent work showed that the specificity for some microbes is low and that some of those can use sugars of the opposite chirality also (Moazeni et al., 2010). Although the dependence on the type of nutrients has not yet been studied in detail, it may be important to allow for a broad range of different ones in an attempt to account for such ambiguities.
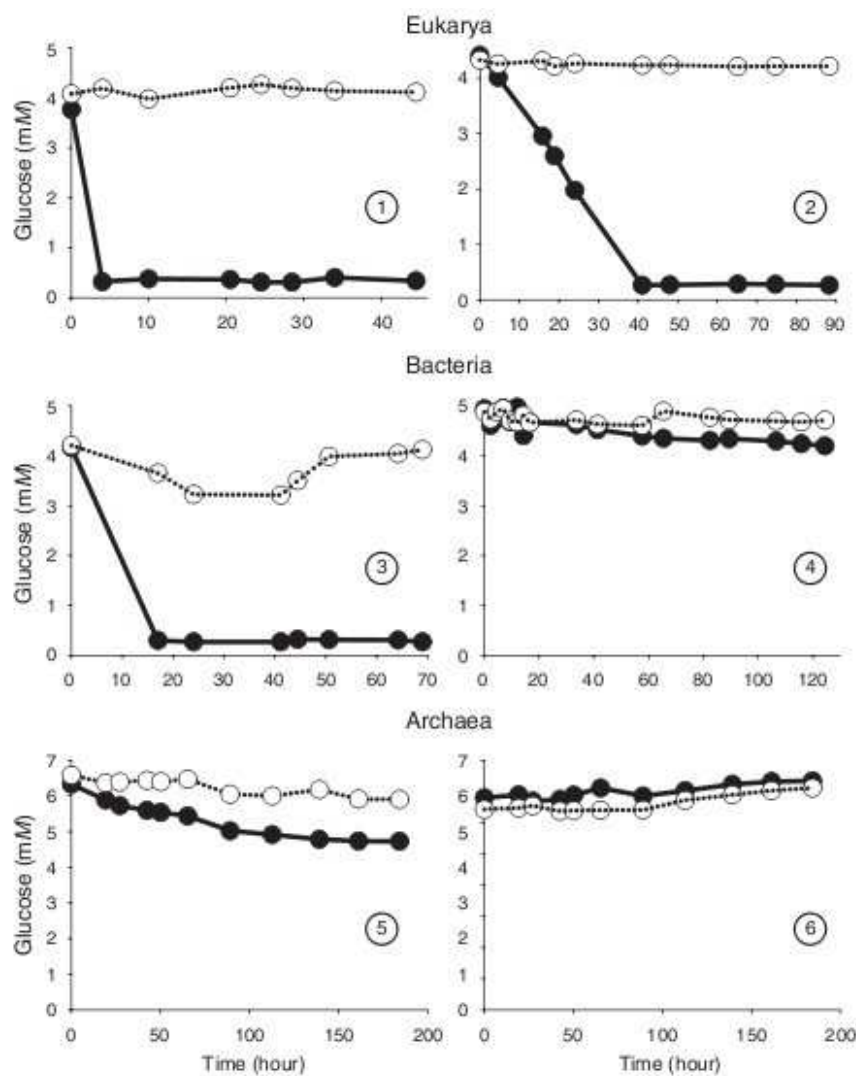
Fig. 4.18 Metabolic consumption of *d* -glucose (filled symbols) and *l* -glucose (open symbols) and by (1) *Saccharomyces cerevisiae*, (2) *Penicilium expansum*, (3) *E. coli*, (4) *Micrococcus luteus*, (5) *Natronobacterium sp.*, and (6) *Halostagnicola sp*. Adapted from Sun et al. (2009).

4.13 Conclusions

Louis Pasteur was well ahead of his time when he identified the biological role of chirality in living matter. Particular remarkable is his realization that,

during fermentation, the metabolic uptake of nutrients of opposite chiralities is different. To understand why this experiment was not put in the context of extraterrestrial life detection, we have to realize that in those years, it was not uncommon to think of extraterrestrial life on Mars. When the astronomer Herschel (1784) discovered seasons on Mars, he wrote in his paper in the Philosophical Transactions of the Royal Society that this "planet has a considerable but moderate atmosphere so that its inhabitants probably enjoy a situation in many respects similar to ours." So, not just the existence of life, but the existence of *intelligent* of life on Mars was commonly expected. This only changed in 1964, when Mariner 4 returned the first flyby pictures of Mars, which suggested that any life there would probably only be of microbial nature. But that Vikings 1 and 2 would not even find any organics on Mars was such a shock to many that the search for life in the Universe appeared fairly hopeless, and Mars exploration was put on hold for the next two decades. This all changed since the turn of the century with the discovery of extremophiles on Earth and the realization that terrestrial life has existed since the time that stable continents existed. Gradually, with the conclusive detection of water on Mars, the search for extinct or extant life on Mars restarted, and Pasteur's discovery of different metabolic uptakes of D and L nutrients may finally turn into an actual Martian experiment. As shown by Sun et al. (2009), this property can be used to detect the presence of homochirality through in situ experiments. Homochirality can also be detected through remote sensing by looking for circular polarization. This approach has been persued by Patty et al. (2019), who found negative or left-handed circularly polarized light emitted from terrestrial plant life at about 680 nm; see also Avnir (2021) for a recent review. To what extent this technique can be used as a biomarker still needs to be seen, but it is amazing to see once more how Pasteur's early discoveries have shaped some important aspects of astrobiology.

While homochirality remains a property that is strongly associated with life—or at least some chemical process that keeps the system far from equilibrium—it is not clear whether we should expect it to have the same or the opposite handedness as an Earth (Bada, 1996). To answer this question, one would need to have more realistic models with meaningful estimates for the concentrations of suitable chemicals in some protocells. This would allow for an estimate of the level of fluctuations in relation to the strengths of the small but systematic effects resulting from the weak force. It would be the only way of guaranteeing that each genesis of life always produces the same chirality. But for now, we should be satisfied if one could find (and understand) any type of an extraterrestrial metabolic process that works differently for nutrients of D and L forms. Thus, the discussed possibilities would need to be put on a quantitatively meaningfully basis. And if it is not life, it certainly is interesting enough to deserve serious attention!

Acknowledgements

References

Anders, E., DuFresne, E. R., Hayatsu, R., Cavaille, A., DuFresne, A., & Fitch, F. W.: 1964, Contaminated meteorite, *Science* **146**, 1157–1161.

Athavale, S. V., Simon, A., Houk, K. N., & Denmark, S. E.: 2020, Demystifying the asymmetry-amplifying, autocatalytic behaviour of the Soai reaction through structural, mechanistic and computational studies, *Nat. Chem.* **12**, 412–423.

Avetisov, V. A., Goldanskii, V. I., & Kuz'min, V. V.: 1991, Handedness, origin of life and evolution, *Phys. Today* **44**, 33–41.

Avnir, D.: 2021, Critical review of chirality indicators of extraterrestrial life, *New Astron. Rev.* **92**, 101596.

Baaske, P., Weinert, F. M., Duhr, S., Lemke, K. H., Russell, M. J., & Braun D.: 2007, Extreme accumulation of nucleotides in simulated hydrothermal pore systems, *Proc. Nat. Acad. Soc.* **104**, 9346–9351.

Bada, J. L.: 1995, Origins of homochirality, *Nature* **374**, 594–595.

Bada, J. L.: 1996, Amino acid homochirality on Earth and Mars, *Orig. Life Evol. Biosph.* **26**, 518–519.

Bailey, J.: 2001, Astronomical sources of circularly polarized light and the origin of homochirality, *Orig. Life Evol. Biosph.* **31**, 167–183.

Bailey, J., Chrysostomou, A., Hough, J. H., Gledhill, T. M., McCall, A., Clark, S., Ménard, F., & Tamura, M.: 1998, Circular polarization in star forming regions: implications for biomolecular homochirality, *Science* **281**, 672–674.

Barge, L. M., Branscomb, E., Brucato, J. R., Cardoso, S. S. S., Cartwright, J. H. E., Danielache, S. O., Galante, D., Kee, T. P., Miguel, Y., Mojzsis, S., Robinson, K. J., Russell, M. J., Simoncini, E., Sobron, P.: 2017, Thermodynamics, disequilibrium, evolution: Far-from-equilibrium geological and chemical considerations for origin-of-life research, *Orig. Life Evol. Biosph.* **47**, 39–56.

Barge, L. M., Flores, E., Baum, M. M., VanderVelde, D. G., Russell, M. J.: 2019, Redox and pH gradients drive amino acid synthesis in iron oxyhydroxide mineral systems, *Proc. Nat. Acad. Soc.* **116**, 4828–4833.

Bonner, W. A., Blair, N. E., & Dirbas, F. M.: 1981, Experiments on the abiotic amplification of optical activity, *Orig. Life* **11**, 119–134.

Bonner, W. A.: 1991, The origin and amplification of biomolecular chirality, *Orig. Life Evol. Biosph.* **21**, 59–111.

Bonner, W. A.: 2000, Parity violation and the evolution of biomolecular homochirality, *Chirality* **12**, 114–126.

Boyd, R. N., Famiano, M. A., Onaka, T., & Kajino, T.: 2018, Sites that can produce left-handed amino acids in the supernova neutrino amino acid processing model, *Astrophys. J.* **856**, 26.

Brandenburg, A.: 2019, The limited roles of autocatalysis and enantiomeric cross-inhibition in achieving homochirality in dilute systems, *Orig. Life Evol. Biosph.* **49**, 49–60.

Brandenburg, A.: 2020, Piecewise quadratic growth during the 2019 novel coronavirus epidemic, *Infectious Disease Modelling* **5**, 681–690.

Brandenburg, A., Andersen, A. C., Höfner, S., & Nilsson, M.: 2005, Homochiral growth through enantiomeric cross-inhibition, *Orig. Life Evol. Biosph.* **35**, 225–241.

Brandenburg, A., Lehto, H. J., & Lehto, K. M.: 2007, Homochirality in an early peptide world, *Astrobiol.* **7**, 725–732.

Brandenburg, A., & Multamäki, T.: 2004, How long can left and right handed life forms coexist? *Int. J. Astrobiol.* **3**, 209–219.

Braun, D., & Libchaber, A.: 2002, Trapping of DNA by thermophoretic depletion and convection, *Phys. Rev. Lett.* **89**, 188103.

Carrier, B. L., Beaty, D. W., Meyer, M. A., Blank, J. G., Chou, L., DasSarma, S., Des Marais, D. J., Eigenbrode, J. L., Grefenstette, N., Lanza, N. L., Schuerger, A. C., Schwendner, P., Smith, H. D., Stoker, C. R., Tarnas, J. D., Webster, K. D., Bakermans, C., Baxter, B. K., Bell, M. S., Benner, S. A., et al.: 2020, Mars extant life: What's next? Conference report, *Astrobiol.* **20**, 785–814.

Cech, T. R.: 1986, A model for the RNA-catalyzed replication of RNA, *Proc. Nat. Acad. Soc.* **83**, 4360–4363.

Cloez, S.: 1864, Note sur la composition chimique de la pierre, *Compt. Rend. Acad. Sci. Paris* **58**, 986.

Davies, P. C. W. & Lineweaver, C. H.: 2005, Finding a second sample of life on Earth, *Astrobiol.* **5**, 154–163.

Derewenda, Z. S.: 2008, On wine, chirality and crystallography, *Acta Cryst.* **A64**, 246–258.

Ehrenfreund, P., Glavin, D. P., Botta, O., Cooper, G., & Bada, J. L.: 2001, Extraterrestrial amino acids in Orgueil and Ivuna: Tracing the parent body of CI type carbonaceous chondrites, *Proc. Nat. Acad. Soc.* **98**, 2138–2141.

Engel, M. H., & Macko, S. A.: 1997, Isotopic evidence for extraterrestrial non-racemic amino acids in the Murchison meteorite, *Nature* **389**, 265–268.

Fajszi, Cs. & Czégé, J.: 1981, Critical evaluation of mathematical models for the amplification of chirality, *Orig. Life* **11**, 143–162.

Frank, F. C.: 1953, On spontaneous asymmetric synthesis, *Biochim. Biophys. Acta* **11**, 459–464.

Gal, J.: 2008, The discovery of biological enantioselectivity: Louis Pasteur and the fermentation of tartaric acid, 1857–A review and analysis 150 yr later, *Chirality* **20**, 5–19.

Gehring, T., Busch, M., Schlageter, M., & Weingand, D.: 2010, A concise summary of experimental facts about the Soai reaction, *Chirality* **22**, E173–E182.

Gilbert, W.: 1986, Origin of life – the RNA world, *Nature* **319**, 618–618.

Gillespie, D. T.: 1977, Exact stochastic simulation of coupled chemical reactions, *J. Phys. Chem.* **81**, 2340–2361.

Gleiser, M., & Walker, S. I.: 2012, Life's chirality from prebiotic environments, *Int. J. Astrobiol.* **11**, 287–296.

Globus, N., & Blandford, R. D.: 2020, The chiral puzzle of life, *Astrophys. J. Lett.* **895**, L11.

Goldanskii, V. I., & Kuz'min, V. V.: 1989, Spontaneous breaking of mirror symmetry in nature and the origin of life, *Sov. Phys. Usp.* **32**, 1–29.

Goldhaber, M., Grodzins, L., & Sunyar, A. W.: 1957, Evidence for circular polarization of bremsstrahlung produced by beta rays, *Phys. Rev.* **106**, 826–828.

Guerrier-Takada, C., & Altman, S.: 1984, Catalytic activity of an RNA molecule prepared by transcription in vitro, *Science* **223**, 285–286.

Hecht, M. H., Kounaves, S. P., Quinn, R. C., West, S. J., Young, S. M. M., Ming, D. W., Catling, D. C., Clark, B. C., Boynton, W. V., Hoffman, J., DeFlores, L. P., Gospodinova, K., Kapit, J., Smith, P. H.: 2009, Detection of Perchlorate and the Soluble Chemistry of Martian Soil at the Phoenix Lander Site, *Science* **325**, 64–67.

Hegstrom, R. A.: 1984, Parity nonconservation and the origin of biological chirality – theoretical calculations, *Orig. Life* **14**, 405–414.

Hegstrom, R. A., Rein, D. W., & Sandars, P. G. H.: 1980, Calculation of the parity nonconserving energy difference between mirror-image molecules, *J. Chem. Phys.* **73**, 2329–2341.

Herschel, W.: 1784, On the remarkable appearances at the polar regions of the planet Mars, the inclination of its axis, the position of its poles, and its spheroidical figure; with a few hints relating to its real diameter and atmosphere, *Phil. Trans. Roy. Soc. Lond.* **74**, 233–273.

Hochberg, D., Bourdon G., Rubén D., Ágreda B, Jesús A., & Ribó, J. M.: 2017, Stoichiometric network analysis of spontaneous mirror symmetry breaking in chemical reactions, *Phys. Chem. Chem. Phys.* **19**, 17618–17636.

Jafarpour, F., Biancalani, T., Goldenfeld, N.: 2015, Noise-induced mechanism for biological homochirality of early life self-replicators, *Phys. Rev. Lett.* **115**, 158101.

Jafarpour, F., Biancalani, T., & Goldenfeld, N.: 2017, Noise-induced symmetry breaking far from equilibrium and the emergence of biological homochirality, *Phys. Rev. E* **95**, 032407.

Joyce, G. F., Visser, G. M., van Boeckel, C. A. A., van Boom, J. H., Orgel, L. E., & Westrenen, J.: 1984, Chiral selection in poly(C)-directed synthesis of oligo(G), *Nature* **310**, 602–603.

Källén, A., Arcuri, P., & Murray, J. D.: 1985, A simple model for the spatial spread and control of rabies, *J. Theor. Biol.* **116**, 377–393.

Klein, H. P., Horowitz, N. H., Levin, G. V., Oyama, V. I., Lederberg, J., Rich, A., Hubbard, J. S., Hobby, G. L., Straat, P. A., Berdahl, B. J., Carle, G. C., Brown, F. S., & Johnson, R. D.: 1976, The Viking biological investigation: Preliminary results, *Science* **194**, 99–105.

Kondepudi, D. K., and Nelson, G. W.: 1983, Chiral symmetry breaking in nonequilibrium systems, *Phys. Rev. Lett.* **50**, 1023–1026.

Kondepudi, D. K., & Nelson, G. W.: 1985, Weak neutral currents and the origin of biomolecular chirality, *Nature* **314**, 438–441.

Konstantinov, K. K., & Konstantinova, A. F.: 2018, Chiral symmetry breaking in peptide systems during formation of life on Earth, *Orig. Life Evol. Biosph.* **48**, 93–122.

Lee, T. D., & Yang, C. N.: 1956, Question of parity conservation in weak interactions, *Phys. Rev.* **104**, 254–258.

Levin, G. V.: 2009, Comment on "Stereo-specific glucose consumption may be used to distinguish between chemical and biological reactivity on Mars: A preliminary test on Earth", *Astrobiol.* **9**, 503.

Levin, G. V., & Straat, P. A.: 1976, Labeled Release – Experiment in radiorespirometry, *Orig. Life Evol. Biosph.* **7**, 293–311.

Levin, G. V., & Straat, P. A.: 1977, Recent results from the Viking Labeled Release Experiment on Mars, *J. Geophys. Res.* **82**, 4663–4667.

Levin, G. V., & Straat, P. A.: 2016, The case for extant life on Mars and its possible detection by the Viking Labeled Release Experiment, *Astrobiol.* **16**, 798–810.

Mason, S. F., & Tranter, G. E.: 1984, The parity-violating energy difference between enantiomeric molecules, *Mol. Phys.* **53**, 1091–1111.

McVoy, K. W.: 1957, Circular polarization of bremsstrahlung from polarized electrons in Born approximation, *Phys. Rev.* **106**, 828–829.

Meierhenrich, U. J., & Thiemann, W. H.-P.: 2004, Photochemical concepts on the origin of biomolecular asymmetry, *Orig. Life Evol. Biosph.* **34**, 111–121.

Miller, S. L.: 1953, A production of amino acids under possible primitive Earth conditions, *Science* **117**, 528–529.

Moazeni, F., Zhang, G., & Sun, H. J.: 2010, Imperfect asymmetry of life: Earth microbial communities prefer D-lactate but can use L-lactate also, *Astrobiol.* **10**, 397–402.

Murray, J. D., Stanley, E. A., & Brown, D. L.: 1986, On the spatial spread of rabies among foxes, *Proc. Roy. Soc. Lond. Ser. B* **229**, 111–150.

Noble, J. V.: 1974, Geographic and temporal development of plagues, *Nature* **250**, 726–728.

Pasteur, L.: 1853, Umwandlung der Weinsäure in Traubensäure. Entdeckung von unwirksamer Weinsäure. Neue Methode der Zerlegung von Traubensäure in Rechts- und in Linksweinsäure, *Ann. Phys.* **166**, 504–509.

Pasteur, L., "Recherches sur les propriétés spécifiques des deux acides qui composent l'acide racémique," In *Annales de chimie et physique* (ed. Paris: Masson), pp. 56–99. 3rd edition, XXVIII (1922).

Patty, C. H. L., ten Kate, I. L., Buma, W. J., van Spanning, R. J. M., Steinbach, G., Ariese, F., & Snik, F.: 2019, Circular spectropolarimetric sensing of vegetation in the field: possibilities for the remote detection of extraterrestrial life, *Astrobiol.* **19**, 1221–1229.

Pizzarello, S., & Cronin, J. R.: 2000, Non-racemic amino acids in the Murray and Murchison meteorites, *Geochimica et Cosmochimica Acta* **64**, 329–338.

Plasson, R., Bersini, H., & Commeyras, A.: 2004, Recycling Frank: spontaneous emergence of homochirality in noncatalytic systems, *Proc. Nat. Acad. Soc.* **101**, 16733–16738.

Plasson, R., "Chemical reaction network," In *Encyclopedia of Astrobiology* (ed. Gargaud, M., et al.), Id. 483. Springer Berlin Heidelberg (2015).

Quinn, R. C., Zent, A. P., Grunthaner, F. J., Ehrenfreund, P., Taylor, C. L., & Garry, J. R. C.: 2005, Detection and characterization of oxidizing acids in the Atacama Desert using the Mars oxidation instrument, *Planet. Space Sci.* **53**, 1376–1388.

Rothery, D. A., Gilmour, I., & Sephton, M. A.: 2008, *An Introduction to Astrobiology*, Cambridge University Press.

Russell, M.: 2006, First life, *Am. Sci.* **94**, 32–39.

Russell, M. J., Barge, L. M., Bhartia, R., Bocanegra, D., Bracher, P. J., Branscomb, E., Kidd, R., McGlynn, S., Meier, D. H., Nitschke, W., Shibuya, T., Vance, S., White, L., Kanik, I.: 2014, The drive to life on wet and icy worlds, *Astrobiol.* **14**, 308–343.

Sandars, P. G. H.: 2003, A toy model for the generation of homochirality during polymerization, *Orig. Life Evol. Biosph.* **33**, 575–587.

Sandars, P. G. H.: 2005, Chirality in the RNA world and beyond, *Int. J. Astrobiol.* **4**, 49–61.

Sevin, A.: 2015, Pasteur and molecular chirality, *Bibnum [Online], Chimie* **459**, 1–10.,

Soai, K., Shibata, T., Morioka, H., & Choji, K.: 1995, Asymmetric autocatalysis and amplification of enantiomeric excess of a chiral molecule, *Nature* **378**, 767–768.

Stich, M., Ribó, Josep M., Blackmond, D. G., & Hochberg, D.: 2016, Necessary conditions for the emergence of homochirality via autocatalytic self-replication, *J. Chem. Phys.* **145**, 074111.

Sugimori, T., Hyuga, H., Saito, Y.: 2008, Fluctuation induced homochirality, *J. Phys. Soc. Jap.* **77**, 064606.

Sugimori, T., Hyuga, H., Saito, Y.: 2009, Fluctuation induced homochirality in an open system, *Phys. Soc. Jap.* **78**, 034003.

Sun, H. J., Saccomanno, V., Hedlund, B., & McKay, C. P.: 2009, Stereospecific glucose consumption may be used to distinguish between chemical and biological reactivity on Mars: A preliminary test on Earth, *Astrobiol.* **9**, 443–446.

Toxvaerd, S.: 2013, The role of carbohydrates at the origin of homochirality in biosystems, *Orig. Life Evol. Biosph.* **43**, 391–409.

Toxvaerd, S.: 2014, Discrete dynamics versus analytic dynamics, *J. Chem. Phys.* **140**, 044102.

Ulbricht, T. L. V.: 1975, The origin of optical asymmetry on Earth, *Orig. Life* **6**, 303–315.

Valdivia-Silva, J. E., Navarro-González, R., de la Rosa, J. McKay, C. P.: 2012, Decomposition of sodium formate and L- and D-alanine in the Pampas de La Joya soils: Implications as a new geochemical analogue to Martian regolith, *Adv. Spa. Res.* **49**, 821–833.

Voosen, P.: 2018, NASA Curiosity rover hits organic pay dirt on Mars: Carbon molecules in rocks from ancient lakebed resemble kerogen, a "goopy" fossil fuel building block on Earth, *Science* **360**, 1055–1055.

Walker, S. I.: 2017, Origins of life: a problem for physics, a key issues review, *Rep. Prog. Phys.* **80**, 092601.

Zeldovich, B. Ya., Saakyan, D. B., & Sobelman, I. I.: 1977, Energy difference between right-hand and left-hand molecules, due to parity nonconservation in weak interactions of electrons with nuclei, *JETP Lett.* **25**, 94–96.